Published December 1, 1984

Spindle Microtubule Dynamics in Sea Urchin Embryos: Analysis Using a Fluorescein-labeled Tubulin and Measurements of Fluorescence Redistribution after Laser Photobleaching

E. D. SALMON, R. J. LESLIE, W. M. SAXTON, M. L. KAROW, and J. R. McINTOSH
Department of Biology, University of North Carolina, Chapel Hill, North Carolina 27514; and Department of Molecular, Cellular, and Developmental Biology, University of Colorado, Boulder, Colorado 80309

ABSTRACT The rate of exchange of tubulin that is incorporated into spindle microtubules with dimeric tubulin in the cytoplasm has been measured in sea urchin eggs by studying fluorescence redistribution after photobleaching (FRAP). Dichlorotriazinyl amino fluorescein (DTAF) has been used to label bovine brain tubulin. DTAF-tubulin has been injected into fertilized eggs of *Lytechinus variegatus* and allowed to equilibrate with the endogenous tubulin pool. Fluorescent spindles formed at the same time that spindles were seen in control eggs, and the injected embryos proceeded through many cycles of division on schedule, suggesting that DTAF-tubulin is a good analogue of tubulin in vivo. A microbeam of argon laser light has been used to bleach parts of the fluorescent spindles, and FRAP has been recorded with a sensitive video camera. Laser bleaching did not affect spindle structure, as seen with polarization optics, nor spindle function, as seen by rate of progress through mitosis, even when one spindle was bleached several times in a single cell cycle. Video image analysis has been used to measure the rate of FRAP and to obtain a low resolution view of the fluorescence redistribution process. The half-time for spindle FRAP is ~19 s, even when an entire half-spindle is bleached. Complete exchange of tubulin in nonkinetochore spindle and astral microtubules appeared to occur within 60–80 s at steady state. This rate is too fast to be explained by a simple microtubule end-dependent exchange of tubulin. Efficient microtubule treadmilling would be fast enough, but with current techniques we saw no evidence for movement of the bleached spot during recovery, which we would expect on the basis of Margolis and Wilson's model (*Nature (Lond.)*., 1981, 293:705)—fluorescence recovers uniformly. Microtubules may be depolymerizing and repolymerizing rapidly and asynchronously throughout the spindle and asters, but the FRAP data are most compatible with a rapid exchange of tubulin subunits all along the entire lengths of nonkinetochore spindle and astral microtubules.

The microtubules of the mitotic spindle are in some form of assembly steady-state with a soluble pool of tubulin subunits (1–3), but the actual pathways of tubulin exchange are unresolved (4–6). The rate of tubulin exchange with nonkinetochore spindle and astral microtubules appears surprisingly rapid (7–9). At metaphase and early anaphase, the assembly of spindle and astral microtubules is near steady state; since the amount of polymer is approximately constant, the rate of tubulin association must equal the rate of dissociation. If polymerization is blocked at metaphase by abrupt treatment with high concentrations of colchicine or colchicine-like drugs, nonkinetochore microtubule depolymerization follows exponential kinetics with a half-time of 6.5 s. This half-time is equivalent to an initial tubulin dissociation rate of 992 dimers/s/microtubule, if the initial average length of nonkinetochore spindle microtubules is 5.5 μm, half the distance between the chromosomes and the spindle poles at metaphase. Independent evidence for rapid dimer-polymer exchange was

Published December 1, 1984

obtained by Wadsworth and Sloboda (9) who injected a fluorescein-labeled tubulin analogue into sea urchin embryos and observed the growth of fluorescent asters at a rate that corresponded to 700 dimers/s.

We felt that we could learn more about the pathways of tubulin exchange within spindle microtubules of living cells by using fluorescent analog cytochemistry (10–13) and techniques for measuring fluorescence redistribution after photobleaching (FRAP) (14–20). In our approach the fluorescent tubulin molecules are used as "tracers" of the cellular tubulin pool—they should assemble and disassemble into spindle microtubules mimicking the behavior of endogenous tubulin subunits. Starting from the work of Keith et al. (21), we have developed a bovine neuro-tubulin analogue labeled with dichlorotriazinyl amino fluorescein (DTAF). Evidence so far available indicates that the DTAF-tubulin is a satisfactory analogue to native tubulin in vitro (22). In reassembly buffers it has similar polymerization-depolymerization characteristics as unlabeled tubulin. When assembly is nucleated with fragments of flagellar axonemes, fluorescent microtubules grow from the ends of the axonemes; no fluorescent tubulin is seen binding to the walls of the axonemes. The growth pattern of fluorescent microtubules from centrosomes and on asters indicates an equilibrium exchange of tubulin subunits at the ends of the microtubules, as expected for microtubule assembly in vitro (23, 24). In this and the following report, we extend these observations to show normal changes in the assembly and disassembly of fluorescent mitotic spindle and interphase microtubules during numerous cell cycles following microinjection of DTAF-tubulin into sea urchin embryos and into cultured mammalian cells (25).

FRAP techniques exploit the susceptibility of the fluorochrome label to permanent bleaching by exposure to light (14–20). Furthermore, with laser microbeaming, fluorescence can be bleached in restricted, well-defined regions of a cell. Because photobleaching of the fluorochrome is permanent (14–16), recovery of fluorescence in a bleached region of the spindle or astral complex requires a redistribution of unbleached, labeled tubulin subunits into the irradiated area. A preceding paper describes the instrumentation and video image analysis procedures we have developed for quantitating temporal changes in the spatial distribution of fluorescence in living cells and presents measurements of the diffusion coefficient of DTAF-tubulin in sea urchin embryos (26).

For the experiments reported here, we injected DTAF-tubulin into sea urchin embryos before first mitosis so labeled tubulin dimers would be incorporated throughout the microtubules that formed the mitotic spindle. Then, at metaphase, we irradiated part of the spindle with a laser microbeam, bleaching the fluorescence of the DTAF-tubulin in the irradiated area. We know that extensive depolymerization of microtubules did not occur, because bleaching did not change the birefringent retardation of the spindle. Thus for fluorescence to recover in the bleached part of the spindle, the bleached DTAF-tubulin subunits in the microtubules of the spindle fibers must be exchanged with other, nonirradiated DTAF-tubulin subunits. In this report we describe and analyze the redistribution of fluorescence of mitotic spindles in sea urchin embryos after the photobleaching. Companion papers report similar photobleaching experiments for microtubules assembled in vitro (22) and for microtubules of mitotic spindles and the cytoplasmic microtubule complex in living mammalian cells in culture (25).

MATERIALS AND METHODS

Reagents: Tubulin was prepared from beef brain and labeled with dichlorotriazinyl amino fluorescein (DTAF) as described earlier (22, 26). The DTAF stocks were stored at 2–4 mg/ml as 10-μl samples in liquid N_2. Fluorescein isothiocyanate-labeled BSA (FITC-BSA), the generous gift of Michael Zavortink (University of Colorado at Boulder), had a dye-to-protein ratio of about 2. It was stored at −20°C as a 4 mg/ml stock in 10 mM PO_4, pH = 7.0 buffer. Nocodazole was obtained from Janssen Pharmaceutical Co. (Piscataway, NJ).

Injection of Eggs and Embryos: Eggs and embryos of *Lytechinus variegatus* were cultured in a Kiehart-Ellis "wedge" chamber, and injected as described in Salmon et al. (26). The wedge chamber flattens these 115-μm-diam cells to ~75 μm in the dimension parallel to the microscope optic axis. About 0.5 h before injection, a 10-μl stock of DTAF-tubulin was thawed and dialyzed into injection buffer (20 mM Na-glutamate, pH 6.8, 1 mM $MgCl_2$, 1 mM EGTA, 0.5 mM GTP) at 4°C, and stored on ice. For FITC-BSA injections, the stock solution was diluted 1:8 into injection buffer. We injected 15–40 embryos about 15 min after fertilization. Injection volumes were estimated from the diameter of the bolus of injected fluid immediately following injection. From these numbers and the dimensions of the unflattened egg, we estimate that the volume of our injected samples ranged from 1–3% of the total cell volume.

Fluorescence Microscopy, Photobleaching, and Video Recording: The instrumentation for fluorescence microscopy, laser photobleaching, low light level video photography, and quantitation of fluorescence intensity distributions by densitometry of negatives taken of the video monitor are described in a preceding paper (26).

In a typical spindle photobleaching experiment, our procedure was as follows: (*a*) The location of the focused laser beam, attenuated by a 3 OD neutral density filter, was marked on the video monitor by the position of the laser beam's fluorescence on a piece of double-stick Scotch brand tape. (*b*) Under dim, whole-field epi-illumination, greatly attenuated to minimize photobleaching, the specimen was positioned so that the spindle area to be bleached was centered at the mark on the video monitor and brought into focus. (*c*) Whole field epi-illumination was used to record a 0.5-s exposure of the specimen field through the TV camera onto 35-mm film before bleaching. (*d*) Photobleaching was performed with the full power of the laser. (*e*) Using full field epi-illumination, 0.5-s photographic recordings of the video monitor were made within 1 s after completion of the photobleach and at various intervals thereafter to record recovery. Shutters blocked the epi-illumination between exposures to minimize whole-field photobleaching. We have shown that the bleaching introduced by the illumination necessary for recording by low light level video photography was negligible as long as no more than ten 0.5-s photographs of the video monitor were made.

Analysis of Fluorescence Redistribution after Photobleaching: We measured the amount of fluorescence in different regions of the spindle and the cell with densitometry of the 35-mm films made by photographing the video monitor (26). Negatives were scanned on a Joyce-Loebl Model 3C scanning microdensitometer. The slit length chosen was about one-third the breadth of the metaphase plate on the negative to be scanned. The slit width was about one-twentieth the distance pole-to-pole on the negative, corresponding to the size of one pair of video scan lines. Each negative was scanned from the unexposed negative background on one side of the cell, passing down the pole-to-pole axis of the spindle and off the cell into unexposed negative background on the other side.

The relation between optical density on the film, as measured by densitometry, and light intensity at the specimen plane was calibrated by using a small, transparent copy of a Kodak gray scale standard, as described in reference 26. By using a Venus DV2 video camera at full manual gain and maintaining fixed settings of both the pedestal and monitor controls, we achieved a system with a linear output of OD for a linear input over a 0.95 OD range. We worked within this range. An Apple II Plus computer and a Houston Instruments Hi-Pad digitizier (Austin, TX) allowed us to digitize the OD tracings and compute the antilogarithm to get specimen fluorescence intensity as a function of position. This curve we assumed to represent the concentration of fluorochrome as a function of position in the cell.

For each experiment, the regions of the optical density tracings corresponding to cytoplasm away from the spindle were aligned to normalize for over-all bleaching of the cell during photographic exposures and laser photobleaching. Total amounts of fluorescence in a given region were estimated with a computer program that measured the area under a fluorescence intensity curve between two chosen spatial boundaries along the spindle interpolar axis. The relative amount of fluorescence at different times could be established easily with this method. These relative amounts at successive times in a given half-spindle region were used to describe the rates of fluorescence redistribution after

Published December 1, 1984

photobleaching. The prebleach value was normalized to 1.0, and other values were expressed as fractions. In general, the fluorescence $FN_{(t)}$ was at a minimum immediately after bleaching, FN_0, and then increased exponentially towards an asymptotic value, FN_∞. The recovery of fluorescence in the spindle is about 18 times slower than expected for the diffusion of tubulin into the spindle region (see Discussion). We characterized the exponential recovery of fluorescence in bleached regions of spindle and astral microtubules by using the perturbation-relaxation equation:

$$FN_{(t)} = FN_0 + (FN_\infty - FN_0)(1 - e^{-kt}), \quad \text{Eq. 1}$$

where $FN_{(t)}$ is the total fluorescence in a given region at any time t after the bleach, and k is a constant describing the rate of recovery. In the spindle experiments, FN_0 was measured 1–1.5 s after bleaching. The time for recovery half way from FN_0 to FN_∞, ($t_{1/2}$), is given by

$$t_{1/2} = \ln 2/k. \quad \text{Eq. 2}$$

FN_0 was taken to be the first fluorescence intensity measured after the bleach (usually within 1 s). FN_∞ and k were determined by fitting a curve of the form shown in Eq. 1 to the data for recovery by the method of least squares. The partial derivative of the sum squared error expression from Eq. 1 with respect to FN_∞ can be evaluated at minimum error and the result used to write the other partial derivative as a function of k only. The roots of the equation formed by setting this derivative = 0 were found numerically by the method of bisection and used to determine best values for both $t_{1/2}$ and FN_∞ for each data set.

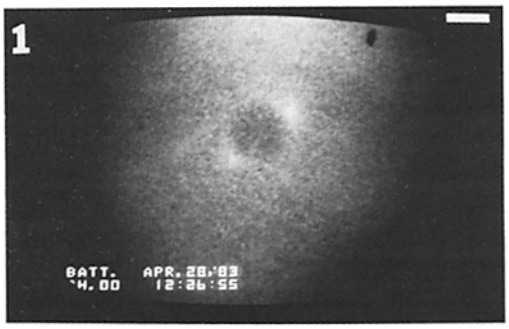

FIGURE 1 Photograph from the video monitor of the DTAF-tubulin distribution at prophase. Astral regions on opposite sides of the nucleus are prominent in the first mitotic embryo. A similar pattern was observed at prophase of later divisions. Bar, 20 μm. × 275.

RESULTS

Incorporation of DTAF-tubulin into Spindle and Astral Fibers

Our interpretation of the photobleaching experiments assumes that the DTAF-tubulin is actually incorporated into the spindle microtubules without altering normal spindle assembly or mitotic events. The following evidence supports the assertion that this assumption is valid.

At each mitosis following fertilization, the distribution of DTAF-tubulin fluorescence in the cell follows the pattern expected for microtubule assembly during the cell cycle (Figs. 1–2). In all experiments reported here, DTAF-tubulin was injected into fertilized eggs 15–20 min post-fertilization, the time of fusion of the male and female pronuclei. Fluorescence became uniformly distributed throughout the cell, but appeared to be excluded from the nucleus. About 20 min later, at experimental temperatures of 23–25°C, bright fluorescent spots appeared at either end of the nucleus, which corresponded to the formation of the prophase asters (Fig. 1) (27, 28). Following nuclear membrane breakdown, fluorescence intensity increased rapidly as the spindle formed (Fig. 2, *a* and *b*). Note, at anaphase, the drop in fluorescence in the spindle equatorial region as the half-spindles separate and shorten. Note also the characteristic expansion of the asters during anaphase and telophase. Apparently normal fluorescent mitotic figures have been observed even in 128-cell stage embryos that were injected with DTAF-tubulin before first division (data not shown).

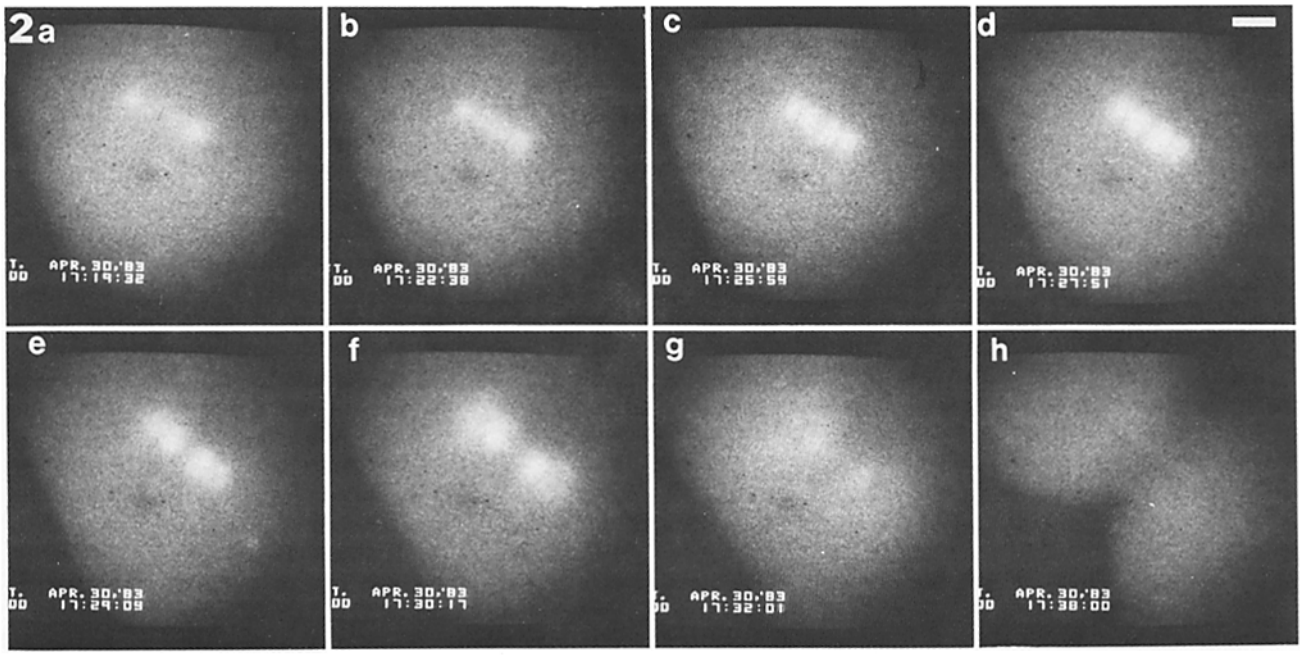

FIGURE 2 Photographs from the video monitor of the DTAF-tubulin distribution from prometaphase through telophase and cell cleavage in a first division embryo. Full metaphase occurs near 17:25:54 while anaphase onset occurred about 17:27:30. Note the distinct fluorescence of the half-spindle in metaphase and anaphase and that the fluorescence of the asters is distinctly separate dfrom the fluorescence of the half-spindles. Individual astral and half-spindle fibers are not visible, in part because of the light-scattering produced by the yolk and because of the low resolution of the low light level video camera. Time in hours:minutes:seconds is given in the lower lefthand corner of each frame. Bar, 20 μm. × 275.

Published December 1, 1984

The intracellular concentration of DTAF-tubulin was an important factor, however, for successful mitosis. We observed some abnormalities if the amount of DTAF-tubulin injected was greater than ~10% of the estimated total intracellular tubulin. The central spindles were brightly fluorescent, but metaphase spindles were shorter than normal, had small asters, and showed little astral growth during anaphase and telophase (Fig. 3). Karyokinesis was successful in these embryos, but cleavage generally was not (data not shown). Furrowing usually initiated only if a spindle was situated close to the cell surface. At later times in embryogenesis, these uncleaved embryos contained multiple nuclei. As a control, we injected fertilized eggs with about one-tenth the cell volume of injection buffer containing 1 mg/ml FITC-BSA. This had no effect on spindle assembly, cleavage, or development followed as far as gastrulation. The toxic effect of high concentrations of DTAF-tubulin may be related to its origin from mammalian brain. At 23–25°C in the sea urchin cytoplasm, the rate at which the mammalian brain tubulin associates could be less than that of embryonic sea urchin tubulin. We have not yet investigated whether unlabeled tubulin has an effect similar to that of DTAF-tubulin. Since spindle assembly and embryonic development were apparently normal with low concentrations of DTAF-tubulin, we were careful to keep the amounts of DTAF-tubulin injected low enough to avoid any observable adverse effects.

If the intensity of fluorescence in the spindle region is due to the polymerization of DTAF-tubulin into spindle microtubules, then depolymerization should result in a loss of fluorescence intensity. Fig. 4 demonstrates that cells that were perfused with high concentrations of nocodazole lost astral and most half-spindle fluorescence within ~30 s. Previous experiments with high concentrations of drugs like nocodazole, such as colchicine, have shown that when tubulin polymerization is abruptly blocked, the astral and nonkinetochore half-spindle microtubules depolymerize in 15–25 s (7, 8). The more stable kinetochore microtubules (7, 8), which represent 10–20% of the total number of normal metaphase half-spindle microtubules (29, 30), persist. Thus the weakly fluorescent central spindle that remains after nocodazole treatment probably represents the remaining kinetochore microtubules. An additional conclusion from these results is that co-polymerization of DTAF-tubulin with the endogenous tubulin does not significantly alter the normal rate of tubulin dissociation from astral and nonkinetochore spindle microtubules.

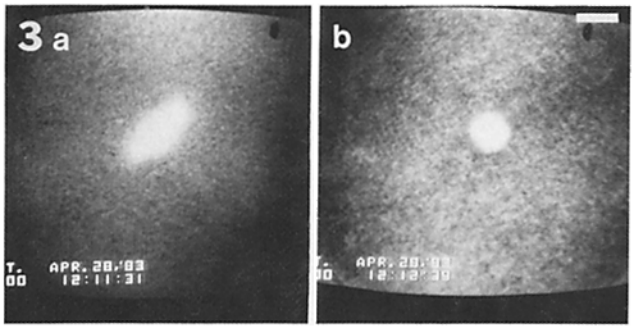

FIGURE 3 Fluorescence (*a*) and polarization micrographs (*b*) of a first division mitotic cell previously injected with high concentrations of DTAF-tubulin. At high DTAF-tubulin concentrations, short, brightly fluorescent spindles with small asters form. Fluorescence and polarization micrographs are taken as described in the text. Bar, 20 μm. × 275.

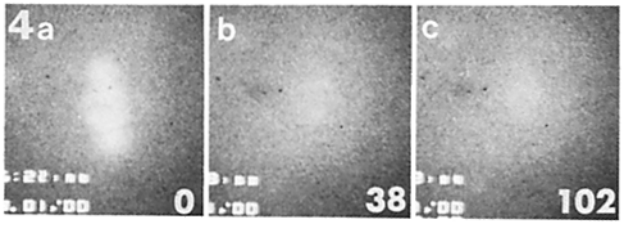

FIGURE 4 Disappearance of nonkinetochore fiber spindle and astral fluorescence following addition of nocodazole to block microtubule polymerization. This metaphase cell was sprayed with sea water containing 10 μg/ml nocodazole from a micropipette at time = 0. Time in seconds following nocodazole treatment is given in each frame. Within 38 s, only a weakly fluorescent central spindle and clear zone are visible above the cytoplasmic background fluorescence. During the nocodazole spraying, the cell rotated clockwise by ~40°. × 275.

Most of the DTAF-tubulin fluorescence in the spindle region is due to the high concentration of assembled microtubules. The peak fluorescence intensity in the metaphase half-spindle region is 1.6–2.0 times the fluorescence observed in adjacent cytoplasmic regions when the cell is injected with DTAF-tubulin. In comparison, FITC-BSA injections led to a ratio of 1.1–1.2 for metaphase spindle fluorescence relative to background. Wang and Taylor (31) previously noted that the yolk-free "clear zone," in which the spindle and aster complex is located, has a slightly higher concentration of fluorescent BSA than the surrounding cytoplasm. The large yolk granules, which are excluded from the clear zone, probably cause a greater dispersion of FITC-BSA molecules in the cytoplasm than in the clear zone, resulting in a lower level of fluorescence. Thus some of the fluorescence intensity seen in the spindle region of sea urchin embryos may be due to a higher concentration of DTAF-tubulin dimers or small oligomers in the clear zone (Fig. 4, 38-s frame), but most is due to the concentration of DTAF-tubulin in spindle and astral microtubules.

Spindle microtubules are known to reassemble rapidly following transient depolymerization by a variety of physical and chemical agents (1–3, 32, 33). We examined the possibility that the laser photobleaching might reversibly depolymerize the spindle microtubules by measuring changes in spindle birefringence after cell irradiation. The birefringent retardation (BR) of spindle fibers has been shown to be proportional to the number of microtubules along the optical path (34, 35). The epi-fluorescence microscope was modified to allow rapid switching of optical components from polarization transmitted light microscopy to epi-fluorescence microscopy, without having to move the specimen or the stage. After taking photographs of the birefringence and fluorescent images, we bleached the spindle fluorescence by laser irradiation, and the birefringent image was viewed within the 6–7 s it took to shift optical components. Within that time, we saw no change in the magnitude nor distribution of spindle birefringence (Fig. 5). No effect of laser photobleaching on spindle birefringence nor on the rate of mitosis and completion of cleavage was seen in four other similar experiments, even when a fluorescent spindle was bleached while viewed continuously in polarization optics. The lack of effect of bleaching on spindle function was particularly evident in experiments during which one cell of a two or four-cell embryo was repetitively bleached while the other cells were left unperturbed. Three bleaches to ~50% initial fluorescence

Published December 1, 1984

followed by recovery had no observable effect on the rate of mitosis in the bleached cell compared with the unbleached sisters. Thus the laser photobleaching does not cause spindle microtubules to depolymerize as does ultraviolet microbeaming (36).

Fluorescence Redistribution after Photobleaching (FRAP)

When fluorescence was photobleached over large or small regions of the spindle-aster complex, the recovery of fluorescence intensity in the bleached region had four striking characteristics (Figs. 5–8): it was exponential, rapid, uniform, and nearly complete. The recovery of fluorescence conformed to an exponential function of time after photobleaching (Fig. 6). The half-time, $t_{1/2}$, and asymptotic value, FN_∞, of recovery could be estimated by fitting the data with a single, exponential perturbation-relaxation function (Eqs. 1 and 2). The $t_{1/2}$ for 50% recovery of fluorescence was 19.4 ± 6.2 s (number of samples, n = 14). Recovery was generally complete within 60–80 s. The relative amount of initial fluorescence bleached was NF_0 = 0.6 ± 0.1 (n = 14). The asymptotic value of fluorescence recovery, FN_∞, for metaphase spindles was 0.93 ± 0.05 of the initial fluorescence (n = 14), though the measurements of FN_∞ are not completely reliable for sea urchins because the extent of microtubule assembly changes during the course of mitosis, which continues normally during fluorescence redistribution. Frequently spindles photobleached in late metaphase progressed into mid-anaphase by the time fluorescence recovery was well advanced (see Figs. 7 and 8). In addition, whole-cell bleaching occurred during each exposure to the fluorescence-exciting light necessary for image recording. The accumulated effect of the exposures tended to reduce both the magnitude of the fluorescence and the signal-to-noise ratios at later recovery times. Following each photobleach, the spindle recovered most of the prebleach fluorescence within 60–80 s; the rate of fluorescence recovery appeared to be independent of the size of the bleached region in the spindle-aster complex. During recovery, fluorescence intensity increased uniformly within the region bleached. We could detect no distinctive spatial pattern to the recovery seen on the video images (Figs. 7 and 8) or the densitometric recovery profiles (Fig. 6). Thus there was no apparent directionality to the recovery of fluorescence. We hesitate, however, to eliminate the possibility of transport phenomena occurring during fluorescence recovery from these observations, because space resolution is limited by the long bleaching periods (2–8 s), the large size of the bleaching spot relative to the 11-μm length of the half-spindle, the light-scattering by cytoplasmic yolk granules, and the low signal-to-noise ratio of the video imaging system.

DISCUSSION

At the concentrations we have used, DTAF-tubulin appears to incorporate into spindle microtubules with normal assembly characteristics. Mitosis and development proceeded as expected in the embryos and, as demonstrated in the companion paper (18), in cultured mammalian cells as well. We think we can legitimately assume that the distribution of fluorescence observed in the sea urchin cells reflects the natural distribution of endogenous tubulin molecules. There are two additional critical assumptions in our use of FRAP to measure normal microtubule dynamics in living cells: (*a*) the DTAF-tubulin polymerizes only into microtubules and not onto the walls of microtubules formed by the endogenous tubulin; and (*b*) photobleaching DTAF that is bound to tubulin incorporated into microtubules does not significantly affect normal microtubule structure and assembly-disassembly. Available evidence supports these assumptions. In reas-

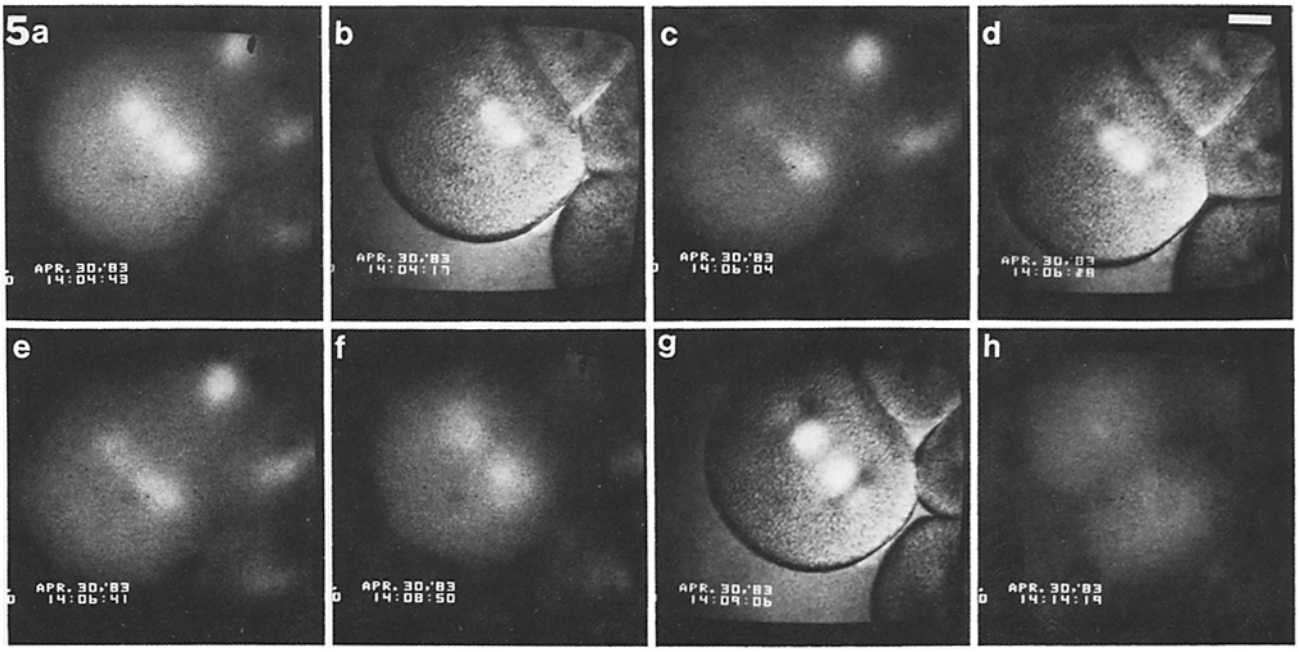

FIGURE 5 Fluorescence and polarization micrographs demonstrating that photobleaching does not significantly alter the normal amount and distribution of spindle and astral fiber birefringence, the morphological changes in assembly during mitosis, nor the timing of mitotic events. Frames *a*, *c*, *e*, *f*, and *h* are fluorescence micrographs and frames *b*, *d*, and *g* are polarization micrographs. Time in hours:minutes:seconds is given in the lower lefthand corner of each frame. Bleaching for 8 s with a 12-μm diam laser beam ended at 14:06:03. Bar, 20 μm. × 275.

Published December 1, 1984

sembly buffer in vitro, DTAF-tubulin was not observed to bind to the walls of microtubules in flagella axonemes nor in asters (22); end-dependent microtubule growth was observed (22). Also, the rate at which DTAF-tubulin is incorporated into microtubules in living cells is proportional to the lability of the microtubules. In mammalian culture cells the more stable interphase cytoplasmic microtubules incorporate DTAF-tubulin at about 1/20 the rate of labile mitotic spindle microtubules (25). The rates of FRAP in cytoplasmic and labile mitotic microtubules show a similar difference (25). Fluorescence recovery was extremely slow (10%/h) after the photobleaching of asters which had been assembled in vitro by nucleating microtubule polymerization of DTAF-tubulin on purified centrosomes (22). This very slow rate of fluorescence recovery is expected for a simple equilibrium exchange of tubulin subunits at the distal ends of astral microtubules (24, 37) and not for tubulin exchange at sites all along the length of the microtubules.

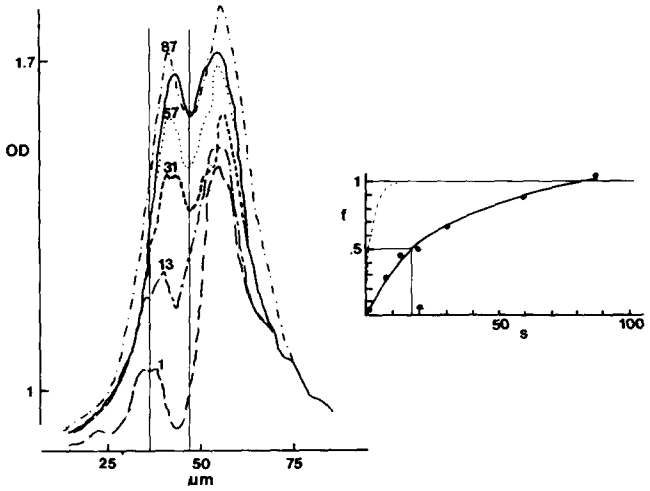

FIGURE 6 Quantitative analysis of the recovery of fluorescence in the photobleached metaphase half-spindle of Fig. 10. The curves in *a* are tracings of optical density scans along the spindle interpolar axis of the photographic negative exposures from the video monitor. Time, *t*, in seconds, is indicated on each curve, with time = 0 at the end of the 4-s photobleaching period. The vertical lines are separated by 10 μm and enclose the half-spindle region which was bleached. To measure the time-dependence of fluorescence during recovery in the bleached half-spindle $F(t)$, optical density curves for each exposure time, *t*, were digitized into an Apple computer, converted to fluorescence intensities as described in the Materials and Methods, and integrated over the 10 μm half-spindle region. Values of $F(t)$ were normalized by the half-spindle fluorescence before bleaching, $F(-)$, giving $FN(t)$. In *b*, $FN(t)$ is plotted against the recovery time, *t*, for the experiment in *a*. Here the characteristic time for 50% recovery of fluorescence is 18 s. The solid line through the data points was derived from Eq. 1, where $k = 0.06\ s^{-1}$ as described in the text. Note that at 90-s postbleach, the half-spindle fluorescence exceeds the prebleach half-spindle fluorescence. This occurs because the spindle has progressed into anaphase where the total amount of half-spindle microtubule polymer is greater than at metaphase (see Fig. 2 and the text for details).

Our photobleaching protocol did not induce extensive disassembly of spindle microtubules in sea urchin embryos as shown both by polarization optical measurement of spindle BR and fluorescence optical measurement of mitotic rate. No microtubule depolymerization was observed after photobleaching fluorescent microtubules in culture cells (25) or in vitro (22). Photobleaching can cross-link and inactivate microtubule proteins in vitro under some conditions (22, see also reference 14). The possibility that photobleaching does submicroscopic damage to the tubulin lattice has not yet been ruled out. Dislocations of the tubulin lattice in microtubule walls would not be observable with the polarization optics we have used to test for microtubule integrity, nor with antitubulin immunofluorescence microscopy (25), nor by electron microscopy of negatively stained microtubules in vitro (22). Since, however, multiple laser photobleaches did not alter spindle morphology nor the cells' progression through mitosis, we have no indication that laser photobleaching altered the structure or function of spindle microtubules in vivo. The current evidence is positive that our FRAP protocol measures steady-state microtubule dynamics.

Even when relatively large areas of the spindle and aster were irradiated, recovery of fluorescence had a half-time of ~20 s and was complete within 60–80 s. The rate of recovery of spindle fluorescence is not limited by the rate of tubulin diffusion into the spindle region, but is limited by the rate of incorporation of tubulin into the spindle. The half-time for recovery of fluorescence due to two-dimensional, isotropic cytoplasmic diffusion is given approximately by:

$$t_{1/2} = \omega^2/4D, \qquad \text{Eq. 3}$$

where ω is the radius of a cylindrical bleached region and D is the diffusion coefficient (15, 16). For $\omega = 5$ μm, corresponding to the radius of the bleached region of the half-spindle in

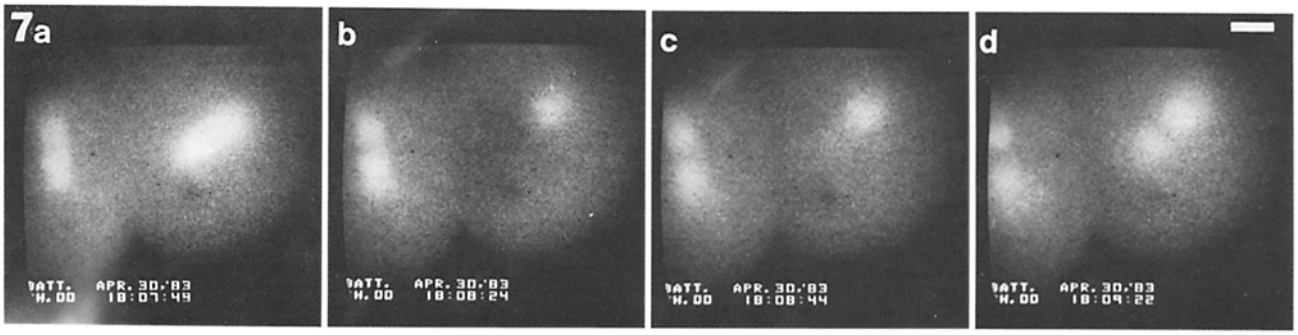

FIGURE 7 Recovery of fluorescence following photobleaching of one half-spindle and aster in a second division embryo with 12-μm diam laser beam. Photobleaching at about anaphase onset for 4 s ended at 18:08:23. Recovery of fluorescence occurs as spindle progresses through anaphase. Note that the recovery of spindle and astral fluorescence is substantial within 60 s. The bleaching does not delay the normal morphological changes in the spindle and aster which occur in anaphase as can be seen by comparing the progression of the bleached and unbleached spindles. Time is given in hours:minutes:seconds at bottom lefthand corner of each frame. Bar, 20 μm. × 275.

Published December 1, 1984

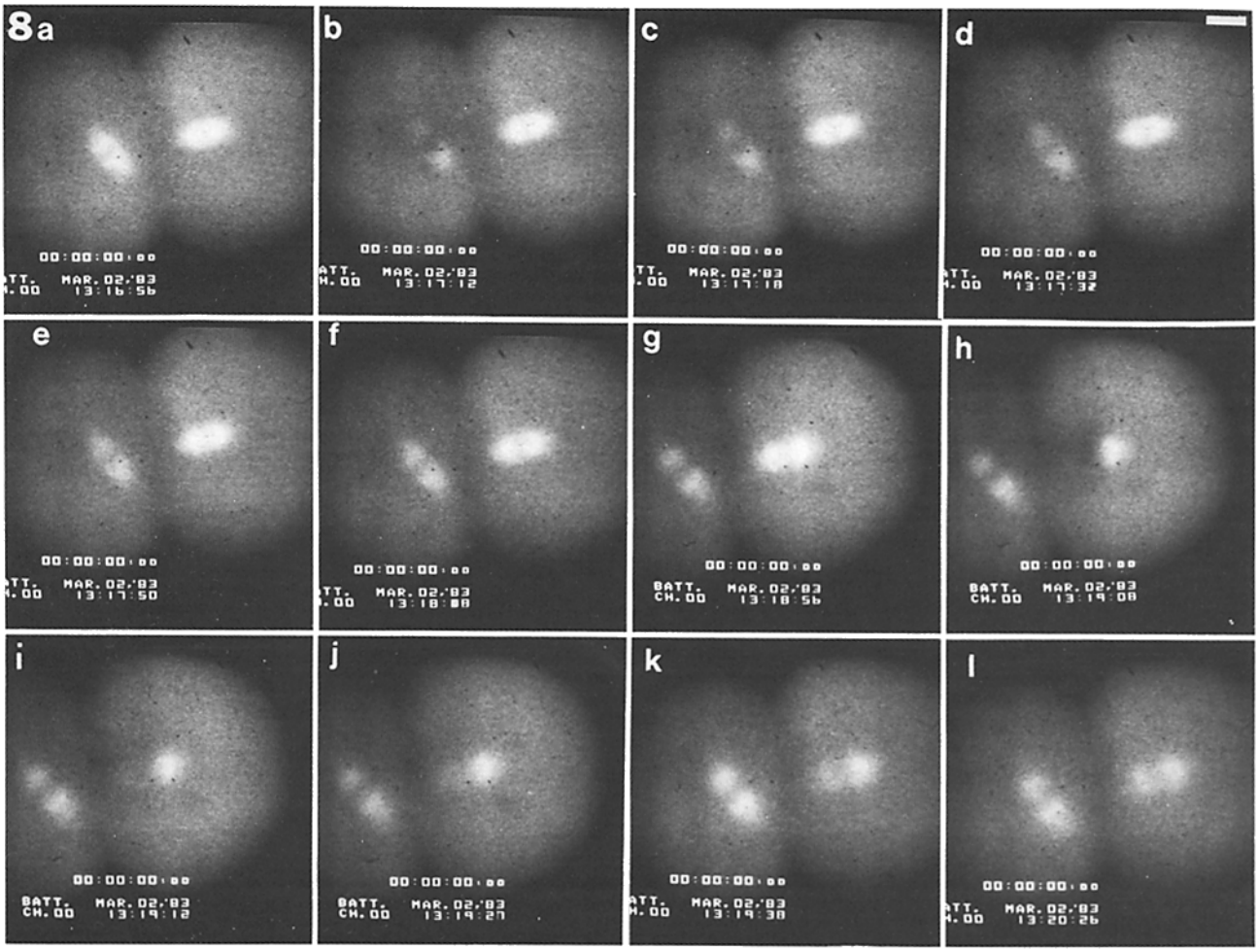

FIGURE 8 Fluorescence recovery after photobleaching a half-spindle in a second-division, metaphase spindle, and in the sister spindle in anaphase. In each case, photobleaching was accomplished with a 4-μm diam laser beam. Time in hours:minutes:seconds is given on each frame. For the metaphase spindle, the 4-s bleach ended at 13:17:11 and for the sister spindle, in anaphase, the 4-s bleach ended at 13:19:07. Between 13:18:09.5 and 13:18:16 the cells were repositioned on the microscope stage to align the anaphase half-spindle with the axis of the focused laser beam. Because the sensitivity of the low light level camera varies across the video field (called "shading"), the relative intensity of the specimen changes with repositioning of the specimen in the video field. Note that in both metaphase and anaphase, recovery of normal fluorescence intensity in the half-spindle occurs over ~60 s. Mitotic timing was normal: both cells cleaved to form a four-cell embryo. The recovery of fluorescence in the bleached metaphase half-spindle is analyzed quantitatively in Fig. 7. Bar, 20 μm. × 275.

Figs. 6 and 8, and $D^{25^\circ}_{tub} = 6 \times 10^{-8}$ cm^2/s, as measured for the cytoplasm of the sea urchin embryo (26), $t_{1/2}$ will be ~1 s. The $t_{1/2}$ for 50% recovery of fluorescence was 19 s, ~18 times slower than the rate expected for the recovery of fluorescence by diffusion of DTAF-tubulin into the bleached region (dashed line in Fig. 6*b*). In our experiments, the first photographs were taken 1–1.5 s after photobleaching. Thus only the tail-end of the diffusion component of fluorescence recovery can just be seen in Figs. 7 and 8 in the photographs immediately following photobleaching. Based on the above evidence, we conclude that at steady-state nearly all the tubulin subunits that make up the nonkinetochore spindle and astral microtubules are replaced by new tubulin molecules, including DTAF-labeled subunits from the cellular pool, within 60–80 s. Kinetochore microtubules represent 10–20% of the number of half-spindle microtubules (29, 30), but incomplete recovery of fluorescence, expected from the differential stability of kinetochore microtubules (9), was not observable in our studies due to normal changes in spindle assembly during mitosis and noise in fluorescence intensity data. The distribution of microtubule lengths in sea urchins is not known, but plausible estimates indicate that the average microtubule is at least 1 μm long, but more likely, 5.5 μm long, one-half the distance between poles and chromosomes at metaphase (8, 29, 30). These estimates imply that there are ~1,635–9,000 dimers that must be replaced in each microtubule within 1–1.5 min.

What pathways of tubulin association and dissociation could effect a complete exchange of subunits in nonkinetochore and astral microtubules every 60–90 s? And furthermore, what pathways of assembly-disassembly would produce the exponential fluorescence increase and the uniform spatial distribution of fluorescence recovery that we observed? A sketch of the current concept of microtubule arrangements in the metaphase sea urchin spindle is presented in Fig. 9*a*. This cartoon is based on detailed structural studies (8, 29, 30, 38–43), but is not literal fact and must be taken simply as indicative of the true state of affairs. Polarity studies have shown that astral, nonkinetochore and kinetochore microtubules have a (+) distal polarity pointing away from the cen-

Published December 1, 1984

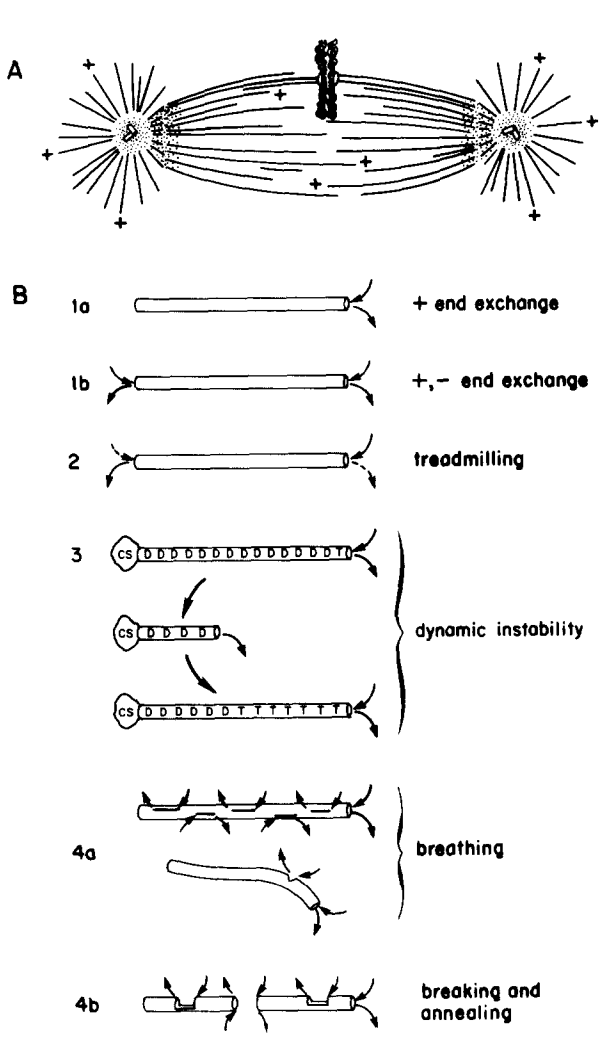

FIGURE 9 (a) Schematic drawing of the apparent microtubule distribution in spindles and asters of metaphase and early division embryonic sea urchin cells; and (*b*) diagrams that illustrate the major proposed pathways for tubulin subunit exchange within spindle microtubules. Details are given in the text. Dots in *a* and *CS* in *b* represent microtubule organizing material associated with the centrosome and spindle poles.

trosome or spindle poles (42, 43).

Fig. 9*b* illustrates four proposed pathways for tubulin subunit exchange between spindle microtubules and the cellular tubulin pool. In the first scheme (Fig. 9*b*, *1*), subunit exchange occurs by reversible association-dissociation events at either one or both ends of a microtubule (23, 24, 44). The observed 60–80 s turnover of tubulin within the spindle cannot be explained by this mechanism alone. The average number of tubulin dimers, m, replaced inward from one end of a microtubule as a function of time, t, by simple equilibrium exchange, is given by

$$m = 2(k_d t/\pi)^{1/2}, \qquad \text{Eq. 4}$$

where k_d is the dimer dissociation rate constant (24, 37). If k_d = 180–992 dimers/s, corresponding to an average spindle microtubule length of 1–5.5 μm (7, 8), m = 117–225 dimers replaced in 60 s. Even if we assume that simple equilibrium exchange occurs at both ends of a microtubule simultaneously, at most only 14% of the tubulin dimers could be replaced in 60 s. The end exchange model does not explain tubulin dynamics in microtubules in living cells, but this model does predict the slow recovery of fluorescence observed after photobleaching fluorescent asters in vitro (22).

Treadmilling, or head-to-tail polymerization, is theoretically much more efficient as a mechanism of subunit exchange (Fig. 9*b*, *2*) (6, 23, 24, 45–48). In the scheme proposed by Margolis et al. (6, 45), tubulin dimers would assemble preferentially at microtubule "plus" ends, the ends distal to the spindle poles or centrosome complex, while they would disassemble preferentially at proximal, "minus" ends. To exchange all the tubulin dimers in a microtubule 1–5.5 μm long within 60 s, the rate of head-to-tail polymerization would have to be 27–148 dimers/s as discussed above. Based on k_d = 180–992 dimers/s, the efficiency of treadmilling would have to be ~15% to account for the measured rate of microtubule turnover. This corresponds to a Wegner head-to-tail polymerization parameter, s = 0.15 (24). Although values of s reported for the assembly of microtubule protein purified from brain and axonemes are small (24, 47) ($s < 0.10$), the efficiency of subunit flux for microtubules assembled from purified brain tubulin is s = 0.26 (48). No kinetic data are yet available for the in vitro assembly of tubulin purified from sea urchin embryo cytoplasm, but high efficiency head-to-tail polymerization could in principle account for the 60–80 s exchange of tubulin within nonkinetochore spindle and astral microtubules.

The Margolis et al. treadmilling model of microtubule assembly and function in the mitotic spindle (6, 45, 46) predicts, however, that we should see a translation of the bleached region towards the spindle poles during fluorescence recovery. We have not seen such a pattern of fluorescence recovery in spindles of sea urchin embryos, nor in spindles of mammalian culture cells (25), but the resolution and signal-noise ratios of our imaging system are not yet of sufficient quality for us clearly to eliminate this treadmilling model for tubulin association-dissociation in mitotic spindles. If distribution of both (−) and (+) ends and of the lengths of microtubules occurs randomly throughout the half-spindle, then treadmilling could produce rapid, uniform, and exponential recovery of fluorescence. However, the generation of chromosome movements by treadmilling, as proposed by Margolis et al. (6, 44, 45), requires that the (−) end of half-spindle microtubules be anchored near the spindle poles.

Mitchison and Kirschner (4) have recently found evidence that whole microtubules can turn over rapidly in a population of microtubules at steady-state assembly (Fig. 9*b*, *3*). The hydrolysis of GTP, bound to tubulin at the ends of microtubules, is thought to regulate rapid, catastrophic depolymerization of entire microtubules (4, 49). If nonkinetochore spindle and astral microtubules are continuously depolymerizing, then regrowing from the centrosomes, as this model proposes, our FRAP results indicate that this process must occur rapidly, but asynchronously among the population of microtubules with a half-time of ~20 s. When assembly is blocked, nonkinetochore spindle microtubules depolymerize extremely rapidly, with a half-time of 6.5 s (8), as required by this model. A major reservation for this proposed mechanism concerns limitations on the required rates of microtubule polymerization, which are discussed in detail elsewhere (8). The possible rate of end-dependent microtubule elongation appears too slow. This conclusion is based on the highest estimated tubulin concentration in the sea urchin embryo, and the largest

rate constant measured for end-dependent association of tubulin in vitro (corrected for rate of tubulin diffusion in the cytoplasm). For these conditions in the sea urchin cytoplasm (8), a microtubule will elongate only 0.66 μm within the 20 s half-time of fluorescence recovery (e.g., 27 μm $\times$ 2 $\times$ 10^6 M^{-1} s^{-1} $\times$ 20 s/1,635 dimers μm^{-1} = 0.66 μm).

The fourth possibility illustrated in Fig. 9*b* is that tubulin subunits exchange at sites all along the length of spindle microtubules (1, 3, 50). This could occur by some form of lattice "breathing" and intercalation of subunits. Or microtubules could be rapidly breaking and reannealing, with simple equilibrium exchange of tubulin subunits occurring at the broken ends (51). In either case, the rate of recovery of fluorescence after photobleaching would be a product of the amount of bleached fluorescence and the average rate constant for dimer dissociation per unit length of a microtubule. This situation should result in exponential kinetics of fluorescence recovery, as described by Eq. 1. The FRAP data for both sea urchin and mammalian spindles is characterized well by Eq. 1 within the limited accuracy of the data. The depolymerization of nonkinetochore spindle microtubules that occurs when polymerization is abruptly blocked with high colchicine concentrations also follows exponential kinetics. The half-time of depolymerization is 6.5 s^{-1}, about 1/3 the half-time of fluorescence recovery that we measured in our FRAP studies. Thus the rates of tubulin dissociation from spindle microtubules determined by these two different methods are comparable. The uniform pattern of fluorescence recovery is also consistent with the exchange of tubulin subunits all along the apparent length of the spindle microtubules. However, we do not have, nor do we know of, any direct evidence that tubulin can exchange at sites other than microtubule ends. In vitro, microtubules assemble and disassemble exclusively by addition and deletion of subunits from the microtubule ends (4, 23, 24). Perhaps in the living cell as yet unidentified microtubule-associated proteins sever microtubules or disrupt the tubulin lattice in a manner analogous to the action of some proteins on actin filaments (52).

In summary, the results of our FRAP experiments support the idea that tubulin exchange with spindle microtubules at steady-state assembly in the living cell occurs too rapidly to be explained by the simple equilibrium exchange of subunits at the ends of spindle microtubules 1–5.5 μm long. The substantial recovery of fluorescence in bleached areas of the spindles within 60–90 s indicates that nearly all tubulin subunits that make up the nonkinetochore and astral spindle microtubules are replaced by tubulin subunits from the cellular pool in this short period. Microtubule treadmilling, as proposed by Margolis et al. (6, 45, 46), could be fast enough to explain the rapid rate of fluorescence recovery, but the predicted poleward transport of the bleached region has not been observed. The rapid and random catastrophic dismantling and regrowth of spindle fiber microtubules, as proposed by Mitchison and Kirschner (4), could explain the uniform pattern of fluorescence recovery, but current kinetic parameters for microtubule elongation in vivo are not consistent with this scheme. The rapid exponential increase and the apparent uniformity of the fluourescence throughout the irradiated area during recovery are both consistent with the hypothesis that tubulin subunits exchange all along the length of spindle microtubules.

This work was performed in the laboratory of J. R. McIntosh while E. D. Salmon was there on sabbatical leave. The latter wishes to thank the former for an enjoyable and productive stay in his lab. We are grateful to Ken Jacobson, Pat Wadsworth, and Lans Taylor for their superb advice and stimulating discussions. Thanks also to Nancy Salmon for her usual excellent editorial assistance.

We appreciate the generous loan of lasers from the following institutions: a model 136 argon laser from Spectraphysics, Mountain View, CA; a model 1 argon laser from Lexel, Inc., Fort Worth, TX; and a Liconix model 4050 He-Cd laser from the San Francisco Laser Center, Department of Chemistry, University of California, Berkeley, CA. Research supported by National Institutes of Health GM 24364 to E. D. Salmon and National Institutes of Health GM 31213 to J. R. McIntosh.

Received for publication 13 March 1984, and in revised form 9 August 1984.

REFERENCES

1. Inoué, S., and H. Sato. 1967. Cell motility by labile association of molecules. *J. Gen. Physiol.* 50:259–292.
2. Salmon, E. D. 1975. Spindle microtubules: thermodynamics of in vivo assembly and role in chromosome movement. *Ann. NY Acad. Sci.* 253:383–406.
3. Inoué, S. 1981. Cell division and the mitotic spindle. *J. Cell Biol.* 91(No. 3, Pt. 2):131s–147s.
4. Mitchison, T. J., and M. W. Kirschner. 1984. Dynamic instability of microtubule growth. *Nature (Lond.).* In press.
5. McIntosh, J. R. 1979. Cell division. *In* Microtubules. K. Roberts, and J. S. Hyams, editors. Academic Press, Inc., New York. pp 428–441.
6. Margolis, R. L., and L. Wilson. 1981. Microtubule treadmills—possible molecular machinery. *Nature (Lond.).* 298:705–711.
7. Salmon, E. D., M. McKeel, and T. Hays. 1982. The rapid rate of tubulin dissociation from microtubules in the mitotic spindle in vivo. *J. Cell Biol.* 95:309*a*. (Abstr.)
8. Salmon, E. D., M. McKeel, and T. Hays. 1984. The rapid rate of tubulin dissociation from microtubules in the mitotic spindle in vivo measured by blocking polymerization with colchicine. *J. Cell Biol.* 99:1066–1075.
9. Wadsworth, P., and R. D. Sloboda. 1983. Microinjection of fluorescent tubulin into dividing sea urchin eggs. *J. Cell Biol.* 97:1249–1254.
10. Wang, Y., J. M. Heiple, and D. L. Taylor. 1982. Fluorescent analog cytochemistry of contractile proteins. *Methods Cell Biol.* 25:1–11.
11. Taylor, D. L., P. A. Amato, K. Luby-Phelps, and P. McNeil. 1984. Fluorescent analog cytochemistry. *Trends Biochem. Sci.* 9:88–91.
12. Kreis, T., and W. Birchmeier. 1982. Microinjection of fluorescently labeled proteins into living cells with emphasis on cytoskeletal proteins. *Int. Rev. Cytol.* 75:209–227.
13. Wang, K., J. R. Feramisco, and J. F. Ash. 1983. Fluorescent localization of contractile proteins in tissue culture cells. *Methods Enzymol.* 85:514–562.
14. Jacobson, K., E. Elson, D. Koppel, and W. Webb. 1983. International workshop on the application of fluorescence photobleaching techniques to problems in cell biology. *Fed. Proc.* 42:72–79.
15. Axelrod, D., D. E. Koppel, J. Schlessinger, E. Elson, and W. W. Webb. 1976. Mobility measurement by analysis of fluorescence photobleaching recovery kinetics. *Biophys. J.* 16:1055–1069.
16. Jacobson, K., Z. Dersko, E.-S. Wu, Y. Hou, and G. Poste. 1976. Measurement of the lateral mobility of cell surface components in single, living cells by fluorescence recovery after photobleaching. *J. Supramol. Struct.* 5:565–576.
17. Wojcieszyn, J. W., R. A. Schlegel, E.-S. Wu, and K. A. Jacobson. 1981. Diffusion of injected macromolecules within the cytoplasm of living cells. *Proc. Natl. Acad. Sci. USA.* 78:4407–4410.
18. Kreis, T. E., Geiger, and J. Schlessinger. 1982. Mobility of microinjected rhodamine actin within living chicken gizzard cells determined by fluorescence photobleaching recovery. *Cell.* 29:835–845.
19. Wang, Y.-L., F. Lanni, P. L. McNeil, B. R. Ware, and D. L. Taylor. 1982. Mobility of cytoplasmic and membrane-associated actin in living cells. *Proc. Natl. Acad. Sci. USA.* 79:4660–4664.
20. Lanni, F., D. L. Taylor, and B. R. Ware. 1981. Fluorescence photobleaching recovery in solutions of labeled actin. *Biophys. J.* 35:351–364.
21. Keith, C. H., J. R. Feramisco, and H. Shelanski. 1981. Direct visualization of fluorescein-labeled microtubules in vitro and in microinjected fibroblasts. *J. Cell Biol.* 88:234–240.
22. Leslie, R., W. M. Saxton, B. Neighbors, T. Mitchison, E. D. Salmon, and J. R. McIntsoh. 1983. Assembly properties of fluorescein-labeled tubulin in vitro before and after photobleaching. *J. Cell Biol.* 99:2146–2156
23. Scheele, R. B., and G. G. Borisy. 1981. In vitro assembly of microtubules. *In* Microtubules. K. Roberts and J. S. Hyams, editors. Academic Press, Inc. New York. 175–252.
24. Hill, T., and M. Kirschner. 1982. Bioenergetics and kinetics of microtubule and action filament assembly-disassembly. *Int. Rev. Cytol.* 78:1–125.
25. Saxton, W. M., D. L. Stemple, R. J. Leslie, E. D. Salmon, M. Zavortink, and J. R. McIntsoh. 1983. Tubulin dynamics in cultured mammalian cells. *J. Cell Biol.* 99:2175–2186.
26. Salmon, E. D., W. Saxton, R. Leslie, M. L. Karow, and J. R. McIntosh. 1983. Diffusion coefficient of fluorescein-labeled tubulin in the cytoplasm of embryonic cells of the sea urchin *Lytechinus variegatus*: measurement by video image analysis of fluorescence redictribution after photobleaching. *J. Cell Biol.* 99:2157–2164.
27. Harris, P., M. Osborn, and K. Weber. 1980. Distribution of tubulin containing structures of the sea urchin *Strongylocentrotus purpuratus* from fertilization through first cleavage. *J. Cell Biol.* 84:668–679.
28. Balczon, R., and G. Schatten. 1983. Microtubule-containing detergent extracted cytoskeletons in sea urchin eggs from fertilization through cell division: Antitubulin immunofluorescence microscopy. *J. Cell Motility.* 3:213–226.

29. Salmon, E. D., and R. R. Segall. 1980. Calcium-labile mitotic spindles isolated from sea urchin eggs (*Lytechinus variegatus*). *J. Cell Biol.* 86:355–365.
30. Harris, P. 1975. The role of membranes in the organization of the mitotic apparatus. *Exp. Cell Res.* 94:409–425.
31. Wang, Y., and D. L. Taylor. 1979. Distribution of fluoresently labeled actin in living sea urchin eggs during early development. *J. Cell Biol.* 82:672–679.
32. Inoué, S., J. Fuseler, E. D. Salmon, and G. W. Ellis. 1975. Functional organization of mitotic microtubules. Physical chemistry of the in vivo equilibrium system. *Biophys. J.* 15:725–744.
33. Sluder, G. 1976. Experimental manipulation of the amount of tubulin available for assembly into the spindle of dividing sea urchin eggs. *J. Cell Biol.* 70:75–85.
34. Sato, H., G. W. Ellis, and S. Inoué. 1975. Microtubular origin of mitotic spindle from birefringence: demonstration of the applicability of Weiner's equation. *J. Cell Biol.* 67:501–517.
35. Hiramoto, Y., Y. Hamaguchi, Y. Shôji, T. E. Schroeder, S. Shimoda, and S. Nakamura. 1981. Quantitative studies on the polarization optical properties of living cells. II. The role of microtubules in birefringence of the spindle of the sea urchin egg. *J. Cell Biol.* 89:121–130.
36. Leslie, R. J. and J. D. Pickett-Heaps. 1983. Ultraviolet microbeam irradiation of mitotic diatoms: investigation of spindle elongation. *J. Cell Biol.* 96:548–561.
37. Zeeberg, B., R. Reid, and M. Caplow. 1980. Incorporation of radioactive tubulin into microtubules at steady-state: Experimental and theoretical analysis of diffusional and directional flux. *J. Biol. Chem.* 255:9891–9899.
38. McIntosh, J. R. 1982. Mitosis and the cytoskeleton. *In* Developmental Order: Its Origin and Regulation. Alan R. Liss, Inc.. New York. 77–115.
39. McIntosh, J. R., W. Z. Cande, and J. A. Snyder. 1975. Structure and physiology of the mammalian mitotic spindle. *In* Molecules and Cell Movement. S. Inoué and R. E. Stephens, editors. Raven Press, New York. 31.
40. MacDonald, K. 1984. Osmium-ferricyanide fixation improves micro filament preservation and membrane visualization in a variety of cell types. *J. Ultrastruct. Res.* 86:107–118.
41. Rieder, C. L. 1982. The formation, structure, and composition of the mammalian kinetochore and kinetochore fiber. *Int. Rev. Cytol.* 79:1–57.
42. Telzer, P. B., and L. T. Haimo, 1981. Decoration of spindle microtubules with dynein: evidence for uniform polarity. *J. Cell Biol.* 89:373–378.
43. McIntosh, J. R., and U. Euteneuer. 1984. Tubulin hooks as probes for microtubule polarity: an analysis of the method and an evaluation of data on microtubule polarity in the mitotic spindle. *J. Cell Biol.* 98:525–533.
44. Kirschner, M. 1980. Implications of treadmilling for stability and polarity of actin and tubulin polymers in vivo. *J. Cell Biol.* 86:330–334.
45. Margolis, R. L., L. Wilson, and B. I. Kiefer. 1978. Mitotic mechanism based on intrinsic microtubule behavior. *Nature* (*Lond.*). 272:450–452.
46. Margolis, R. L. 1978. A possible microtubule dependent mechanism for mitosis. *In* Cell Reproduction. E. R. Dirksen, D. M. Prescott, and C. F. Fox, editors. Academic Press, Inc., New York. 445–456.
47. Farrell, K. W., and M. A. Jordan. 1982. A kinetic analysis of assembly-disassembly at opposite microtubule ends. *J. Biol. Chem.* 257:3131–3138.
48. Cote, R. H., L. G. Bergen, and G. G. Borisy. 1980. Head-to-tail polymerization of microtubules in vitro: a review. *In* Microtubules and Microtubule Inhibitors. M. De Brabander and J. De. Mey, editors. Elsevier/North Holland Biomedical Press, Amsterdam. 325–338.
49. Carlier, M.-F., T. L. Hill, and Y. Chen. 1984. Interference of GTP hydrolysis in the mechanism of microtubule assembly: An experimental study. *Proc. Natl. Acad. Sci. USA.* 81:771–775.
50. Inoué, S., and H. Ritter, Jr. 1975. Dynamics of mitotic spindle organization and function. *In* Molecules and Cell Movements. S. Inoué and R. E. Stephens, editors. Raven Press, New York. 3–30.
51. Bajer, A. S., and J. Mole-Bajer. 1975. Lateral movements in the spindle and the mechanism of mitosis. *In* Molecules and Cell Movement. S. Inoué and R. E. Stephens, editors. Raven Press, New York. 77–96.
52. Bonder, E. M., and M. S. Mooseker. 1983. Direct electron microscopic visualization of barbed end capping and filament cutting by intestinal microvillar 95-kdalton protein (villin): a new actin assembly assay using *Limulus* acrosomal process. *J. Cell Biol.* 96:1097–1107.